

1 **Rhizosphere allocation by canopy-forming species dominates soil CO<sub>2</sub> efflux in a subarctic**  
2 **landscape**

3 Thomas C. Parker (1), Karina E. Clemmensen (2), Nina L. Friggens (1), Iain P. Hartley (3),  
4 David Johnson (4), Björn D. Lindahl (5), Johan Olofsson (6), Matthias B. Siewert (6), Lorna E.  
5 Street (7), Jens-Arne Subke (1) & Philip A. Wookey (1).

6

7 (1) Biological and Environmental Sciences, University of Stirling, Stirling, UK.

8 (2) Swedish University of Agricultural Sciences, Department of Forest Mycology and  
9 Plant Pathology, Uppsala, Sweden.

10 (3) Geography, College of Life and Environmental Sciences, University of Exeter, Exeter,  
11 UK.

12 (4) Department of Earth and Environmental Sciences, University of Manchester,  
13 Manchester, UK.

14 (5) Swedish University of Agricultural Sciences, Department of Soil and Environment,  
15 Uppsala, Sweden.

16 (6) Umeå University, Department of Ecology and Environmental Sciences, Umeå,  
17 Sweden.

18 (7) School of Geosciences, University of Edinburgh, Edinburgh, Scotland, UK.

19

20 **Key Words:** Arctic, girdling, rhizosphere, soil CO<sub>2</sub> efflux, ectomycorrhizal fungi, treeline,  
21 shrub expansion

22

23 **Abstract:**

- 24 • In arctic ecosystems, climate change has increased plant productivity. As arctic  
25 carbon (C) stocks are predominantly located below ground, the effects of greater  
26 plant productivity on soil C storage will significantly determine the net sink/source  
27 potential of these ecosystems, but vegetation controls on soil CO<sub>2</sub> efflux remain  
28 poorly resolved.

- 29
- To identify the role of canopy forming species in below-ground C dynamics, we  
30 conducted a girdling experiment with plots distributed across 1 km<sup>2</sup> of treeline birch  
31 (*Betula pubescens*) forest and willow (*Salix lapponum*) patches in northern Sweden  
32 and quantified the contribution of canopy vegetation to soil CO<sub>2</sub> fluxes and below-  
33 ground productivity.
  - Girdling birches reduced total soil CO<sub>2</sub> efflux in the peak growing season by 53% -  
34 double the expected amount given that trees contribute only half of the total leaf  
35 area in the forest. Root and mycorrhizal mycelial production also decreased  
36 substantially. At peak season, willow shrubs contributed 38% to soil CO<sub>2</sub> efflux in  
37 their patches.
  - Our findings indicate that C, recently fixed by trees and tall shrubs, makes a  
38 substantial contribution to soil respiration. It is critically important that these  
39 processes are taken into consideration in the context of a greening arctic since  
40 productivity and ecosystem C sequestration are not synonymous.  
41  
42

## 43 Introduction

44 Climate warming is causing large-scale increases in primary productivity in much of  
45 the terrestrial Arctic (Myers-Smith *et al.*, 2020), as predicted by long-term warming  
46 experiments (Elmendorf *et al.*, 2012a) and vegetation models (Yu *et al.*, 2017). Where  
47 changes in ecosystem productivity are occurring, they are driven by increased growth of  
48 tundra vegetation (Elmendorf *et al.*, 2012b; Bjorkman *et al.*, 2018), but also often by an  
49 increase in cover and geographical range of deciduous shrub species (Myers-Smith *et al.*,  
50 2011). Above-ground carbon (C) accumulation at northern high latitudes, following  
51 increased productivity, is projected to continue into the next century (Qian *et al.*, 2010).  
52 There is also clear evidence, from responses of trees to historical changes in climate, and  
53 global gradient studies, that arctic and alpine treelines are influenced by climate and that  
54 forests will expand if climate continues to warm (Richardson & Friedland, 2009). Poleward  
55 and altitudinal shifts of treelines have already been observed in some locations (Wilmking *et*  
56 *al.*, 2006; Harsch *et al.*, 2009; Hofgaard *et al.*, 2013; Hagedorn *et al.*, 2014), although  
57 responses are heterogeneous due both to historical and on-going land use and grazing  
58 pressure. Forest expansion in the near future will only influence the tundra close to the  
59 present treeline, but significant increases in productivity have also been observed in large  
60 parts of the low arctic tundra (Reichle *et al.*, 2018). These subzones are found where  
61 deciduous shrub species are present, and often dominant, in the plant community (Walker  
62 *et al.*, 2005). Shrubs in the tundra grow taller and expand their spatial range in response to a  
63 warmer climate (Myers-Smith *et al.*, 2011, 2019a), and are the most likely plant group to  
64 increase in dominance across large areas of the low Arctic in this and the next century  
65 (Pearson *et al.*, 2013).

66 Above-ground biomass in the most productive tundra subzones has increased by up  
67 to 0.1 kg C m<sup>-2</sup> to approximately 0.5 kg m<sup>-2</sup> between 1982 and 2010 (Epstein *et al.*, 2012).  
68 However, this stock of biomass C is small compared to soil C stocks. Tundra soils in the  
69 majority of the treeless Arctic store up to 50 kg C m<sup>-2</sup> and the highest densities of C are  
70 commonly found in the top 30 cm of the profile (Kuhry *et al.*, 2013; Siewert, 2018), along  
71 with almost all of plant root biomass (Jackson *et al.*, 1996; Iversen *et al.*, 2015). This stock  
72 surpasses by far the aboveground C storage even in fully forested boreal (Siewert *et al.*,  
73 2015) and subarctic forests (Hartley *et al.*, 2012). Increasing photosynthetic biomass in the

74 Arctic results in more C entering the ecosystem, and there is much interest in the ecosystem  
75 feedbacks that may result (Myers-Smith *et al.*, 2011, 2019b). However, primary productivity  
76 is just one facet of the terrestrial C cycle, and the fate of assimilated C must also be  
77 understood, on timescales varying from minutes to millennia, to enable a forecasting of  
78 future ecosystem C storage.

79 The task of linking above-ground changes in GPP to total ecosystem storage of C is  
80 complex. Most C fixed by arctic vegetation is allocated below-ground (Street *et al.*, 2018),  
81 where the majority of plant biomass is located (Iversen *et al.*, 2015). GPP can be robustly  
82 characterised in tundra based on leaf area and basic meteorological data (Shaver *et al.*,  
83 2007), meaning that GPP may be predicted by changes in above-ground canopy properties  
84 that can be detected via remote sensing (Epstein *et al.*, 2012). However, the change in  
85 ecosystem respiration with increasing shrub and tree encroachment is much more  
86 challenging to predict. For example, tall deciduous shrub species that are structurally similar  
87 aboveground (*Betula* and *Alnus*) allocate C belowground very differently in relation to  
88 nitrogen acquisition (Street *et al.*, 2018), which may, in turn, affect C turnover rates in the  
89 soil. The fate of photosynthesised C within an ecosystem may therefore differ significantly  
90 between contrasting arctic plant communities.

91 Soil CO<sub>2</sub> efflux constitutes the largest component of ecosystem C losses; in many  
92 forest systems soil CO<sub>2</sub> efflux comprises, in roughly equal measure, of heterotrophic and  
93 autotrophic sources (Bond-Lamberty *et al.*, 2004; Subke *et al.*, 2006). The ratios of  
94 heterotrophic to autotrophic contributions to the total soil CO<sub>2</sub> efflux are less well  
95 characterised in tundra (Shaver *et al.*, 2007; Hicks Pries *et al.*, 2015), but this information is  
96 required in order to understand C budgets. As tall shrubs and trees represent future plant  
97 communities, given further climate change (Pearson *et al.*, 2013), it is particularly important  
98 to quantify and understand their contribution to soil CO<sub>2</sub> efflux within their present  
99 distribution. Quantifying the contribution of recent plant C inputs to soil CO<sub>2</sub> efflux is  
100 technically challenging, usually requiring either destructive methods or isotopic labelling  
101 techniques to partition autotrophic and heterotrophic CO<sub>2</sub> sources (Subke *et al.*, 2006).  
102 Previous trenching and clipping approaches in these ecosystems have caused considerable  
103 disturbance, altered soil thermal and moisture regimes, and have generally only been able  
104 to quantify the total contributions of all vegetation, including short-stature species, to

105 ecosystem fluxes (Hartley *et al.*, 2012). Stem girdling halts the delivery of photosynthate  
106 from canopies to below ground by disrupting the phloem tissue while limiting the reduction  
107 in movement of water to the rest of the plant through the xylem, while leaves remain alive.  
108 This method therefore makes it possible to identify the contribution of canopy-forming  
109 species to soil CO<sub>2</sub> efflux, even where extensive understorey plant communities remain, and  
110 provides a unique insight into the role of canopy species and associated ectomycorrhizal  
111 (ECM) fungi in controlling C fluxes from the soil (Högberg *et al.*, 2001).

112         Alongside plant root respiration, respiration from extraradical ECM mycelium can  
113 contribute 15-25 % of the total soil CO<sub>2</sub> efflux in boreal and temperate forests (Heinemeyer  
114 *et al.*, 2007; Hasselquist *et al.*, 2012; Hagenbo *et al.*, 2019) and ECM mycelial necromass has  
115 been linked with fast decomposition (Drigo *et al.*, 2012; Clemmensen *et al.*, 2015).  
116 Furthermore, low stocks of soil C in treeline forests (compared to adjacent tundra) may be  
117 linked to enzymatic oxidation of organic matter by ECM fungi, as they extract organic forms  
118 of N (Bödeker *et al.*, 2014), and to a broader rhizosphere priming effect by birch trees and  
119 their symbionts (Hartley *et al.*, 2012). In such a system, where canopy-assimilated C is in  
120 high demand for the acquisition of N and other nutrients by symbiotic fungi, a large  
121 proportion of soil CO<sub>2</sub> efflux should be linked to the C supply from the canopy. In contrast,  
122 tundra willow shrub communities typically grow in riparian zones and in areas of deep snow  
123 cover, where soil moisture and mineral nutrient influx is higher than in other tundra types  
124 (Nadelhoffer *et al.*, 1991; Sturm *et al.*, 2005), potentially reducing plant investment in ECM  
125 fungi (Treseder, 2004). Furthermore, high soil moisture and occasional anoxia are not  
126 favourable to many ECM fungi, and can limit their growth within the soil matrix (Lodge,  
127 1989; Wurzburger *et al.*, 2004; Barnes *et al.*, 2018), thus reducing the demand for  
128 assimilated C. Willow shrubs have been widely documented to increase in growth and cover  
129 in response to climate change (Tape *et al.*, 2006; Forbes *et al.*, 2010; Myers-Smith *et al.*,  
130 2019a), therefore it is important to understand C cycling in this ecosystem at present, in  
131 order to predict changes in the future.

132         Flux partitioning experiments have seldom been done in arctic ecosystems (Subke *et*  
133 *al.*, 2006), and the relative influence of the canopy has never been elucidated by girdling.  
134 The problem of partitioning is exacerbated by the diversity and heterogeneity of tundra and  
135 treeline plant communities with contrasting dominant plant species (Walker *et al.*, 2005).

136 Quantitative information on rhizosphere processes in contrasting treeline and tundra plant  
137 communities in relation to plant productivity is essential to underpin a better understanding  
138 of variations in landscape soil CO<sub>2</sub> efflux. To address these issues, we conducted a girdling  
139 experiment at plots across a sub-arctic landscape in northern Sweden to isolate and test the  
140 importance of canopy inputs for soil CO<sub>2</sub> efflux and below-ground productivity.

141 Past experiments that partitioned autotrophic and heterotrophic CO<sub>2</sub> fluxes in boreal  
142 and northern temperate forests, using stem girdling and trenching, were in situations where  
143 the canopy comprised the majority of leaf area (Högberg *et al.*, 2001; Subke *et al.*, 2006). In  
144 a subarctic birch forest, leaf area is likely more equally distributed between canopy and  
145 understorey vegetation. In this forest, trenching canopy roots and clipping the understorey  
146 reduced soil CO<sub>2</sub> efflux by 50 % in peak season (Hartley *et al.*, 2012). We therefore  
147 hypothesised (1) that the contribution by canopy dominant trees to autotrophic soil CO<sub>2</sub>  
148 effluxes would broadly reflect their contribution to the total leaf area of the community.  
149 Furthermore, we hypothesised (2) that autotrophic contribution to soil CO<sub>2</sub> efflux would be  
150 lower under tundra willow than under treeline forest alongside a lower investment in  
151 mycorrhizal fungi.

152

## 153 **Methods**

### 154 *Site selection and experimental design*

155           The experiment was located around a forest-tundra ecotone 3-4 km south of the  
156 Abisko Scientific Research Station, Sweden (68°18 N 18°49 E, ~600 m asl). The girdling  
157 experiment was carried out in mountain birch forest (*Betula pubescens* Ehrh. ssp  
158 *czerepanovii* (Orlova) Hämet Ahti) and willow thickets (Identified as *Salix lapponum* L. but  
159 there is very high potential for hybridisation in this genus (Forrest, 2006)) that were  
160 distributed across a 0.88 km<sup>2</sup> area (Fig. 1). The birch forests grow on well-drained spodosols,  
161 underlain by glacial till without permafrost (Sjögersten & Wookey, 2002). The understorey  
162 primarily comprises of ericaceous dwarf shrubs (*Empetrum nigrum* L. ssp *hermaphroditum*  
163 (Hagerup) Böcher, *Vaccinium myrtillus* L., *Vaccinium vitis-idaea* L. and *Vaccinium uliginosum*  
164 L.) and feather mosses (e.g. *Hylocomium splendens* and *Pleurozium schreberi*) (Fig.S1a).  
165 Willow thickets (Fig.S1b) in this area typically grow in poorly drained, late snow-lie  
166 communities, alongside *Betula nana* L., with an herbaceous and graminoid understorey.

167           Prior to girdling, 5 willow and 6 mountain birch plots were established in early June  
168 2017, with each plot divided into paired sub-plots. Pairs were selected to have similar tree  
169 and stem density, soil C stocks, soil C:N ratio (Table 1) and understorey (birch plots:  
170 ericaceous dwarf shrubs and mosses; willow plots: forbs and mosses). The birch sub-plots  
171 had a circular area with a radius of 10 m and an average tree density of 586 trees ha<sup>-1</sup> (Table  
172 1). The willow sub-plots had a radius of 2 m and a density of 5-6 stems m<sup>-2</sup>, representing the  
173 largest plots with willow-only canopies that could be found in the study area. The larger size  
174 of the birch plots was necessary to ensure that all trees were girdled that could potentially  
175 be contributing to below-ground respiration at the central measurement area. The outer  
176 perimeters of paired birch sub-plots were separated by 10 – 20 m and the paired plots were  
177 separated from other pairs by between 300 to 1100 m (Fig 1a). For the willow plots, the  
178 distances between paired sub-plot outer perimeters were 2 - 16 m and pairs were separated  
179 by between 300 and 900 m. Each birch plot contained 3-4 trees within the central 3 m  
180 radius, within which all subsequent measurements were taken. Unlike in the relatively  
181 sparse birch forest, the lack of gaps between willow shrubs meant that it was also necessary  
182 to trench the perimeter of each willow plot, and plastic sheet was then inserted through the  
183 entire soil depth until rocks were encountered (top 10 – 30 cm of soil) to prevent roots from

184 adjacent plants from entering. Trenching was not carried out around the birch plots,  
185 because the size of the buffering area around the central 3 m radius was deemed sufficient  
186 to minimise edge effects.

187         Soil CO<sub>2</sub> efflux measurements (see Soil CO<sub>2</sub> Efflux section for methods) were carried  
188 out twice at all birch and willow plots after snow-melt (9-12 June 2017) but prior to the  
189 application of girdling treatments. Paired T-tests were carried out to test for a pre-girdling  
190 difference in plot characteristics between sub-plots and no significant differences were  
191 observed (Table 1). One sub-plot of each pair was girdled between 12<sup>th</sup> June 2017 and 15<sup>th</sup>  
192 June 2017. All birch stems over 1 cm in diameter were girdled within the 10 m radius plot. In  
193 the birch plots, a 4-8 cm section of the bark was removed around the circumference of each  
194 stem down to the xylem approximately 30 cm from the ground, leaving no phloem  
195 connection between leaves and roots (Högberg *et al.*, 2001). In the willow plots, every  
196 willow stem was girdled approximately 10-20 cm above the ground. Re-sprouting shoots  
197 from below the girdle-line were removed by hand whenever observed during the  
198 experiment. Birch and willow plants retained leaves until natural senescence in 2017 and all  
199 birch trees produced full leaves above the girdle-line in spring 2018. However, girdled  
200 willow canopies failed to produce leaves in 2018.

201

## 202 *Soil CO<sub>2</sub> Efflux*

203         Two days prior to the first efflux measurement and 5 - 7 days prior to girdling, three  
204 5 cm tall, 15 cm inner-diameter, PVC collars were secured within 1 m of one of the three  
205 central trees of each birch plot. Collars were placed between under-storey stems and areas  
206 of moss mats in order to exclude live above-ground plant material. The collars were pushed  
207 firmly onto the soil and secured to the ground with non-setting plumber's putty (Evo-Stik  
208 Plumber's Mait®), to provide a good seal between collar and soil surface without severing  
209 shallow roots. The same method was applied to willow plots, with three collars placed  
210 within the central 1 m radius of the plot. Effectiveness of the collar seal using plumber's  
211 putty has been demonstrated by a linear increase in CO<sub>2</sub> concentrations when a closed  
212 chamber is attached to the collar (Parker *et al.*, 2015).



213 After girdling, CO<sub>2</sub> efflux was measured on 10 dates in the birch plots and 9 dates in the  
214 willow plots during the 2017 growing season, and 10 times each during the 2018 growing  
215 season. An EGM-5 infrared gas analyser (PP Systems International, Amesbury, MA, USA),  
216 with an attached CPY-5 darkened chamber, was used to measure soil CO<sub>2</sub> efflux (root-  
217 associated and heterotrophic activity). CO<sub>2</sub> efflux was calculated based on the linear  
218 increase in CO<sub>2</sub> concentration over 90 seconds. For each measurement date, all plots were  
219 visited on the same day between the hours of 09:00 and 18:00. The order in which plots  
220 (species and girdling treatment) and collars were sampled was alternated at every sampling  
221 day in order to minimise temporal sampling bias. The average soil CO<sub>2</sub> efflux value from the  
222 three collars was recorded as the true replicate flux per plot.

223

#### 224 *Soil and vegetation characteristics*

225 To understand the effects of girdling on soil CO<sub>2</sub> efflux we measured plant and soil  
226 characteristics in the different plots. Soil organic C stocks of the organic horizon at each plot  
227 were calculated from a mean of nine soil cores (3.8 cm diameter) taken evenly across a 2 × 2  
228 m area in the centre of the plot. The organic horizons from each core were separated from  
229 the lower mineral horizons, mixed together, oven-dried (60 °C) and weighed. C and nitrogen  
230 contents were measured on the combined sample in a Flash Smart™ elemental analyser  
231 (ThermoFisher Scientific, Waltham, MA, USA). Canopy leaf area index (LAI) was measured  
232 using an ACCUPAR LP-80 leaf area meter (Pullman, WA, USA) in early August in 2017 (all  
233 plots) and 2018 (birch plots only). At the birch plots, an average of 20 measurements taken  
234 evenly at 30 cm height across the north-south diameter of the plot was used. In the willow  
235 plots LAI was measured at 30 cm height at five points across the plot. The understory LAI of  
236 each birch forest plot was estimated from the average NDVI of the visible forest floor in the  
237 10 m radius of the plot from a drone platform according to relationships from a previous  
238 remote sensing study at 3 m scale at a nearby forest-tundra ecotone site (LAI = 0.00059  
239 e<sup>9.502</sup> NDVI (R<sup>2</sup> = 0.90) (Williams *et al.*, 2008)).

240 Drone imagery was taken on the 2<sup>nd</sup> August 2017 and 30<sup>th</sup> July 2018 in two flights  
241 using a senseFly eBee mapping drone (senseFly Inc., Switzerland) carrying a Parrot Sequoia  
242 multi-spectral sensor that delivers imagery in four spectral bands (Green, Red, Red Edge,

243 Near Infrared) and a separate RGB orthophoto. The drone was operated at a target  
244 elevation of 106 m resulting in an effective ground resolution of 10.3 cm (2017) and 11.2 cm  
245 (2018) in the final processed raster data of each flight. We used the Pix4Dmapper  
246 photogrammetric software (version 4.2.15, Pix4D, Lausanne, Switzerland) to combine  
247 individual images into continuous raster maps. We extracted an orthophoto and the  
248 normalized difference vegetation index (NDVI), which is considered an indicator of  
249 vegetation abundance and health (Rouse *et al.*, 1974). Each plot was visually marked in the  
250 field and later identified and outlined in the orthophoto composite using 4 m and 20 m  
251 diameter circles for willow and birch plots, respectively. The orthophoto was used to digitise  
252 manually the outline of the canopy of each individual tree in the birch plots and of the  
253 willow shrub coverage in willow plots. For birch plots, we extracted NDVI pixel values for the  
254 most centrally located trees in each plot. Understorey NDVI pixel values per plot were  
255 extracted from within each circle after masking out all tree canopies.

256 With every soil CO<sub>2</sub> efflux measurement from 24<sup>th</sup> July 2017 onwards, conductivity of  
257 the top 5 cm of soil was measured at all plots using a handheld HH2 ThetaProbe soil  
258 moisture meter (Delta-T Devices, Cambridge, UK). In birch plots, measurements were taken  
259 every meter in a 9 m<sup>2</sup> central square grid (16 measurements), and in the willow plots nine  
260 measurements were taken in a 4 m<sup>2</sup> square grid. Soil temperature at 5 cm depth was  
261 measured three times across the grid using a hand-held digital thermometer. Average  
262 temperature and conductivity values were calculated for each plot on each sampling date,  
263 then conductivity was converted to gravimetric moisture content according to:

$$264 \text{ Gravimetric moisture (\%)} = e^{(a+Mb)}$$

265 Where  $M$  is the soil conductivity measured in the field and  $a$  and  $b$  are estimated  
266 based on the fitted relationship between gravimetric moisture and soil conductivity  
267 measured during a dry-down curve of saturated ericaceous peat from near the study plots  
268 ( $a = 4.402$ ,  $b = 0.00129$ , Adjusted  $R^2 = 0.955$ ). Using the bulk density of the calibration soil,  
269 gravimetric moisture was converted to volumetric moisture. To capture continuous  
270 volumetric soil moisture and soil temperature dynamics through timespan of the  
271 experiment, EC 5 soil moisture and TMB temperature smart sensors (Onset, Bourne, MA,  
272 USA) were installed at 5 cm depth in one birch and one willow plot. The probes logged  
273 hourly measurements to HOBO microstation loggers (Onset, Bourne, MA, USA).

274

275 *Growing season root production and birch copy numbers*

276 Root production over the growing season was estimated using ingrowth bags  
277 (Sullivan *et al.*, 2007). Cylindroid fibre-glass mesh bags (6 cm deep and 2.5 x 1.5 cm wide  
278 with a mesh size of 2 mm) were loosely packed with ericaceous peat. The peat was collected  
279 within the study landscape, dried for 48 h at 85°C, and sieved through a 4 mm mesh, with  
280 remaining roots picked out by hand prior to deployment in the bags. Ensuring maximum  
281 contact with the native soil, a root ingrowth bag was inserted vertically into the top six cm  
282 of organic soil, below the litter and moss layers, 30 cm from every CO<sub>2</sub> efflux collar in the  
283 willow and birch plots. Bags remained in the soil from 14<sup>th</sup> June 2017 until 18<sup>th</sup> September  
284 2017, and new bags were inserted from 2<sup>nd</sup> June 2018 until 12<sup>th</sup> September 2018 with a  
285 total of 96 and 102 days field incubation per respective growing season. Bags were retrieved  
286 from the soil by carefully running a scalpel around each bag to a depth of 6 cm. Outside  
287 portions of in-grown roots were cut off in the lab and all roots inside the core were  
288 extracted, washed and dried at 60 °C for 72 hours, after which dry mass was recorded. C  
289 content of the roots was then analysed using a Flash Smart™ elemental analyser.

290 For a species-specific assay, subsamples (0.7 - 30 mg (depending on amounts  
291 remaining after other analyses)) of dried in-growth roots from birch plots were finely milled  
292 by steel nuts (40 s at 5000 rpm) in 2 ml tubes (Precellys, Bertin Instruments, Germany), and  
293 DNA was extracted using the NucleoSpin soil kit (Macherey-Nagel, Düren, Germany). Copy  
294 numbers of the ITS region of *Betula* sp. were analysed by quantitative PCR (qPCR) using  
295 birch-specific primers (ITSb\_F and ITSb\_R) and a Biorad iQ5 real-time PCR detector system  
296 (Bio-Rad, Richmond, CA, USA) according to Pérez-Izquierdo *et al.* (2019). Two 2017 root  
297 samples from girdled plots were not extracted due to lack of sample material at this stage.  
298 Tests with known amounts of plasmid DNA and corresponding M13 primers (Pérez-  
299 Izquierdo *et al.*, 2019), using the same PCR conditions, indicated no significant PCR inhibition  
300 by the root extracts.

301

302 *Hyphal production*

303 Ectomycorrhizal (ECM) fungal hyphal production over the growing season (same dates as  
304 root bags) was estimated using sand-filled ingrowth bags (Wallander *et al.*, 2013). 5 x 5 cm  
305 nylon mesh bags with a 37  $\mu\text{m}$  mesh size were filled with 18 g of sand from Lake Torneträsk  
306 (Parker *et al.*, 2015). The sand was sieved to select particle sizes between 0.125 and 1 mm  
307 and autoclaved twice, then dried at 100 °C for 72 hours. Bags were designed to be thinner  
308 than common practice (only 0.5 cm thick when filled) to limit the distance that mycorrhizal  
309 fungi had to grow in order to colonise the sand, and to encourage fungal groups that may  
310 not typically grow into sand to colonise (Hagenbo *et al.*, 2018). Bags were inserted into the  
311 ground at a 45° angle, directly below the litter layer, 30 cm from each CO<sub>2</sub> efflux collar but  
312 on the opposite side to the root ingrowth cores. Prior to insertion, bags were wetted with  
313 deionised water on a solid surface in order to ensure uniform sand depth across the bag.  
314 Bags remained in the field over the same period as the root bags and blanks were  
315 maintained in the laboratory. Sand was extracted from bags four to six hours after recovery  
316 from the field, frozen at -80 °C, and freeze-dried for 72 hours in a ModulyoD freeze drier  
317 (ThermoFisher Scientific, Waltham, MA, USA). 1.5 g of sand from each bag were sonicated in  
318 25 ml of deionised water for 10 minutes in order to free hyphae from the sand. A 10 ml  
319 aliquot of the hyphae-containing solution was transferred to a Falcon tube, to allow further  
320 separation of hyphae and sand by sedimentation, then transferred into an open container,  
321 dried at 50 °C, weighed and analysed for C content using a Flash Smart™ elemental  
322 analyser. This process was repeated for eight blank samples that had not been deployed in  
323 the field and the average C content was subtracted from all samples.

324

### 325 *Statistical analysis*

326 The effects of girdling, species (willow or birch) and season (early, mid and late) on soil CO<sub>2</sub>  
327 efflux, soil moisture and temperature were analysed using linear mixed effects models with  
328 the nlme package in R (Pinheiro *et al.*, 2016; R Development Core Team, 2016). In the linear  
329 mixed effects model, “plot” was designated as a random variable, to account for the paired  
330 design of the experiment, as was “sub-plot”, to take account of repeated measures. Soil CO<sub>2</sub>  
331 efflux immediately after girdling treatment in June 2017 was not considered in the analysis,  
332 as it was assumed that the treatment had not yet taken effect. All flux data were natural-log  
333 transformed in order to conform to the assumptions of the parametric analysis. The effect

334 of girdling on root and hyphal production, LAI, canopy NDVI and understorey NDVI in birch  
335 and willow plots was also analysed using linear mixed effects models after natural-log  
336 transformation when appropriate (except NDVI, which required arcsine-square root  
337 transformation in order to be appropriate for parametric analysis).

338

339 **Results**

340           Across all plots, birch had significantly higher soil CO<sub>2</sub> efflux rates than willow plots in  
341 2017 ( $P = 0.005$ ; Fig. 2) but not in 2018. Girdling significantly reduced soil CO<sub>2</sub> efflux in both  
342 2017 ( $P < 0.001$ ; Fig. 2) and 2018 ( $P < 0.001$ ; Fig. 2) in birch and willow plots compared to  
343 paired control plots. This reduction in soil CO<sub>2</sub> efflux was large and sustained throughout the  
344 peak seasons of 2017 and 2018. The effect of girdling was maintained into late season  
345 (September), although not as pronounced then as in mid-season. The girdling treatment did  
346 not have a detectably larger effect on soil CO<sub>2</sub> efflux in the birch plots compared to the  
347 willow plots in either year, with a statistically non-significant interaction term between  
348 species and treatment ( $P = 0.38$  and  $P = 0.11$  in 2017 and 2018, respectively; Fig. 2).

349           The girdling treatment allowed for the estimation of ‘canopy-linked’ soil CO<sub>2</sub> efflux  
350 (the difference between control and girdled plots) as a proportion of the total soil CO<sub>2</sub> efflux  
351 in the control plots (Fig. 2, Fig.S2). The remaining proportion of the total flux constituted  
352 respiration of free-living heterotrophs and remaining roots (understorey and canopy species  
353 roots that were still alive). Over the 2017 growing season, the average contribution from  
354 canopy-linked sources to total soil CO<sub>2</sub> efflux in the birch plots was 33 %, but this increased  
355 markedly to 53 % during the peak growing season in early August (Fig. 2, Fig. S2). In 2018  
356 the average canopy-linked contribution to soil CO<sub>2</sub> efflux was again 33 %, with a maximum in  
357 early August of 46 %. The canopy-linked contribution to soil CO<sub>2</sub> efflux in willow shrub plots  
358 was smaller, but still considerable, with an average of 26 % (in 2017) and 21 % (2018), and  
359 maximum contributions of 38 % and 30 %, peaking in early August in each of the respective  
360 years.

361           Girdling significantly reduced total root production compared to control plots in  
362 2017, for birch and willow combined (willow: -30 % change, birch: -75 % change;  $P = 0.009$ ;  
363 Table 2, Fig. 3), with no significant difference between species ( $P = 0.834$ ). This difference  
364 was lost in 2018, with no significant effect of species or girdling treatment on root  
365 production. However, girdling caused a highly significant reduction in birch ITS copy  
366 numbers in ingrowth bags in 2018 ( $P = 0.004$ , Table 2, Fig. 5), with birch root production  
367 decreased to almost zero in girdled plots. Girdling also tended to reduce birch copy numbers  
368 during the first growing season of the treatment (2017) ( $P = 0.079$ , Table 2, Fig. 5).

369           Although birch control plots tended to have higher hyphal production than girdled  
370 plots or willow plots in 2017, there was no overall effect of girdling and only a marginally  
371 significant difference between birch and willow plots ( $P = 0.059$ ; Table 2, Fig. 4). By 2018,  
372 however, there was a highly significant effect of girdling on hyphal production owing 99 %  
373 reduction in girdled birch plots ( $P < 0.001$ ; Table 2, Fig. 4). The lack of difference between  
374 girdled and control in 2018 in willow plots was associated with a significant interaction  
375 between treatment and species ( $P < 0.001$ ).

376           Willow plots had significantly lower NDVI than birch canopy, despite no significant  
377 difference in LAI (Table 2), likely due to the pubescent leaves of *S. lapponum*, which reduce  
378 reflectivity (Street *et al.*, 2007). Girdling significantly reduced canopy NDVI of both species,  
379 but more so in the willow plots, resulting in a significant interaction between species and  
380 treatment (Table 2). In 2017, despite differences in canopy NDVI, LAI remained unaffected  
381 by girdling with no differences between species. In 2018, LAI in girdled birch plots  
382 ( $0.65 \text{ m}^2 \text{ m}^{-2}$ ) dropped significantly below control values ( $0.92 \text{ m}^2 \text{ m}^{-2}$ ) due to reduced birch  
383 leaf development in girdled plots ( $P = 0.024$ , Table 2). Understorey NDVI under birch was  
384 the same between girdled and control plots in both 2017 and 2018, on average remaining at  
385 0.77. The average LAI of the understorey of  $0.88 \text{ m}^2 \text{ m}^{-2}$ , estimated from NDVI according to  
386 the relationship between ground vegetation LAI and NDVI at a 3 m scale at a nearby site ( $\text{LAI}$   
387  $= 0.00059 e^{9.502 \text{ NDVI}}$  (Williams *et al.*, 2008)), indicated that birch trees contribute  
388 approximately half of the leaf area in this ecosystem. It was not possible to make this  
389 calculation in the willow plots due to the resolution of the imagery, making it hard to  
390 differentiate willow and understorey from the drone platform.

391           Soil moisture varied significantly between vegetation types ( $P < 0.001$ , Fig. S3b). In  
392 the growing season of 2017, soil moisture was 1.6 times higher in willow plots than in birch  
393 plots and in 2018 it was 1.5 times higher. There was no statistically detectable effect of  
394 girdling on soil moisture in either year. Both willow and birch plots were exposed to a flush  
395 of water at the time of snow melt in May/June, but soon after soil moisture dropped to  
396 distinctly lower levels in birch plots until soil freeze-up in November (Fig. S3b). Soil  
397 temperature was not different between species or girdling treatment (Fig. S3a).

398

399 **Discussion**

400 Mountain birch forests and willow shrub patches are amongst the most productive  
401 ecosystems in the Fennoscandian subarctic and are representative of plant communities  
402 that are expanding onto tundra as northern latitudes warm (Myers-Smith *et al.*, 2011;  
403 Hofgaard *et al.*, 2013). Although expansion of forest and shrub communities is expected to  
404 increase gross primary productivity there is little understanding of how vegetation change  
405 will influence the C dynamics of the whole system, primarily because the subsequent fate of  
406 assimilated C is so poorly quantified and understood (Street *et al.*, 2018). Here, we use a  
407 girdling experiment to show that recently fixed C contributes 53 % and 33 % (peak season  
408 and full season, respectively) to soil CO<sub>2</sub> efflux in mountain birch communities, and 38 % and  
409 26 % to soil CO<sub>2</sub> efflux in willow communities. The results suggested that much of the C fixed  
410 into these relatively productive ecosystems is rapidly returned to the atmosphere,  
411 constituting a significant fraction of soil CO<sub>2</sub> efflux.

412 We found that leaf area of the birch canopy (measured here at 0.5-0.92 m<sup>2</sup> m<sup>-2</sup>  
413 depending on sampling year) was approximately the same as the leaf area of the  
414 understorey (~0.88 m<sup>2</sup> m<sup>-2</sup> based on conversion from NDVI). The understorey of subarctic  
415 (Kulmala *et al.*, 2019) and boreal (Wardle *et al.*, 2012) forests can contribute 50 % of GPP,  
416 and exclusion of all autotrophic C inputs to the soil in a subarctic birch forest (both canopy  
417 and understorey) resulted in a ~50 % reduction in soil CO<sub>2</sub> efflux at peak growing season  
418 (Hartley *et al.*, 2012). We therefore hypothesised that the contribution from canopy  
419 assimilation to autotrophic soil CO<sub>2</sub> fluxes in mountain birch would reflect its contribution to  
420 community leaf area, which would equate to an approximate 25 % reduction following  
421 girdling given the broadly equal LAI of overstorey and understorey vegetation. Thus, our  
422 finding of a 33 % reduction in soil CO<sub>2</sub> efflux during the growing season following cessation  
423 of inputs from only the birch canopy disagrees with our hypothesis and suggests that birch  
424 makes a larger than expected contribution to soil CO<sub>2</sub> fluxes. In the wider context of  
425 autotrophic-heterotrophic soil CO<sub>2</sub> efflux partitioning (broadly 50 % autotrophic (Subke *et al.*  
426 *et al.*, 2006)), the relative contribution of one species which is only one half of the ecosystem  
427 leaf area is also remarkable.

428 The peak season 53 % reduction in soil CO<sub>2</sub> efflux with girdling in early August  
429 roughly coincides with peak vegetation productivity (Heliasz *et al.*, 2011). Although



430 phenology of peak belowground allocation will vary from year to year, we suggest that  
431 allocation belowground scales with increasing assimilation aboveground. The scale and  
432 seasonality of the canopy-driven soil efflux agrees closely with the results of a previous  
433 girdling experiment in a Swedish boreal forest (Högberg *et al.*, 2001). The Högberg *et al.*  
434 (2001) study was carried out in Scots pine forest (*Pinus sylvestris*) with a sparse understorey  
435 and approximately double the density of trees compared to the present study. Although  
436 there are obvious differences between these ecosystems, our data suggest that mountain  
437 birch trees play a disproportionate role in controlling below-ground C dynamics in these  
438 ecosystems. A girdling treatment in an ericaceous dwarf shrub community (*Calluna vulgaris*)  
439 showed no detectable change in soil CO<sub>2</sub> efflux (Kritzler *et al.*, 2016), indicating that roots  
440 and associated fungi made a much smaller contribution to total soil respiration than in  
441 mountain birch forest. Should trees or shrubs expand onto ericaceous heath, our  
442 experiment suggests that the autotrophic component of soil CO<sub>2</sub> efflux would increase  
443 disproportionately along with increased GPP.

444         The reduction in soil efflux of CO<sub>2</sub> in birch plots after girdling coincided with  
445 reductions in production of birch roots and mycorrhizal mycelium in birch plots,  
446 demonstrating the tight coupling between C assimilation in the canopy, belowground  
447 biomass production and return via soil CO<sub>2</sub> efflux. The reduction in birch root and mycelium  
448 production was greatest in the second year of the treatment with four of six girdled plots  
449 showing zero or near-zero biomass production. This delayed effect suggests that these trees  
450 have a degree of resilience to disturbance, potentially in the form of stored non-structural  
451 carbohydrates that can supplement rhizosphere demand in the short term (Palacio *et al.*,  
452 2008), also supported by some resprouting of shoots below the girdling line. Nevertheless, it  
453 is clear that reduction in C supply from the canopy to the rhizosphere resulted in large  
454 reductions in soil respiration in both birch and willow plots.

455         In 2018, despite the large reduction in birch ITS copy numbers, there was no  
456 significant difference in total root production in the girdled and control plots. We were not  
457 able specifically to estimate ericaceous biomass production directly (because of our lack of  
458 primers targeting the Ericaceae). However, the recovery of overall root productivity,  
459 coupled to the major decline in birch ITS copy numbers, strongly suggests that there was an  
460 increase in root productivity from the ericaceous understorey plants, most likely as a result

461 of these plants being released from competition with the birch trees. In open birch forests,  
462 it is unlikely that shading by the canopy is limiting ericaceous understorey growth; instead,  
463 competition for nutrients may exert a stronger control. In support of this explanation,  
464 invertebrate herbivore events are known to exert a strong control on canopy productivity in  
465 subarctic birch forests (Bjerke *et al.*, 2014) and also increase soil nitrogen availability (Parker  
466 *et al.*, 2017), which, along with frass inputs, is suggested to be driven by reduced uptake by  
467 the birch canopy (Parker *et al.*, 2017). Such disturbance events may release the understorey  
468 from belowground competition and allow for greater ericaceous shrub productivity, as  
469 appears to have occurred in our girdling study. Overall, these findings further demonstrate  
470 the disproportionate role that birch trees play in driving C and nutrient cycling within these  
471 ecosystems, when compared with their contribution to total LAI.

472         The substantial canopy-linked soil respiration flux integrates a number of processes  
473 that occur subsequent to the allocation of photosynthate to the roots. Firstly, roots and  
474 their associated mycorrhizal fungi respire as they grow through the soil (Söderström & Read,  
475 1987; Hagenbo *et al.*, 2019). The second potential source of canopy-linked soil CO<sub>2</sub> efflux is  
476 positive priming of soil organic matter: greater microbial decomposition of soil C as a result  
477 of autotrophic C delivery (Kuzyakov, 2002). Priming has previously been inferred to reduce  
478 soil C storage in mountain birch forests compared to tundra heath, despite high above-  
479 ground biomass and productivity (Hartley *et al.*, 2012). Furthermore, ECM fungi have been  
480 linked to decomposition in boreal, organic-rich soils through the production of extracellular  
481 oxidative enzymes (Lindahl & Tunlid, 2015; Sterkenburg *et al.*, 2018; Zak *et al.*, 2019),  
482 especially when mineral nitrogen availability is low (Bödeker *et al.*, 2014). Therefore,  
483 priming of organic matter by tree and shrub roots and associated mycorrhizal fungi could  
484 contribute a significant fraction of the large canopy-linked soil CO<sub>2</sub> efflux.

485         It is clear that more mycorrhizal hyphae were produced in the birch plots than in the  
486 willow plots and that girdling dramatically reduced this production to almost zero.  
487 Respiration by mycorrhizal hyphae can contribute from 14 to 26 % of total soil CO<sub>2</sub> efflux in  
488 boreal forest (Hasselquist *et al.*, 2012; Hagenbo *et al.*, 2019) and is likely to contribute a  
489 significant fraction of the canopy-linked flux in our mountain birch plots. Furthermore, non-  
490 melanised mycorrhizal necromass is known to degrade rapidly (Wilkinson *et al.*, 2011; Drigo  
491 *et al.*, 2012; Fernandez *et al.*, 2019) and ECM-dominated soils correlate with high soil

492 turnover rates and low soil C compared to ericoid mycorrhizal-dominated systems  
493 (Clemmensen *et al.*, 2015; Parker *et al.*, 2015). Therefore, we expect that, in areas of the  
494 tundra where soils are dominated by ECM symbioses, fungal symbionts play an important  
495 role in the rapid return of autotrophic C as soil CO<sub>2</sub> efflux.

496         The girdling experiment demonstrates a significant contribution of the willow shrub  
497 canopy to soil CO<sub>2</sub> efflux. At its peak, canopy-linked soil CO<sub>2</sub> efflux in willow plots reached  
498 38 % of the total flux. Willows belong to a genus of shrubs that are well documented to be  
499 expanding in the Arctic, garnering significant interest in their associated ecosystem  
500 feedbacks (Myers-Smith *et al.*, 2011, 2019b). Shrubby ecosystems in the tundra have  
501 previously been linked to fast turnover of below-ground C (Parker *et al.*, 2015; Sørensen *et*  
502 *al.*, 2018) and leaf litter (Demarco *et al.*, 2014; Parker *et al.*, 2018), but with this experiment  
503 we were able to quantify soil CO<sub>2</sub> efflux directly driven by recent canopy C assimilation. We  
504 hypothesised that girdling would cause a larger relative reduction in soil CO<sub>2</sub> efflux in birch  
505 than in willow plots as a result of higher allocation of C to mycorrhizal networks in the  
506 former. Indeed it is clear that more mycelium was produced in birch plots, and we observed  
507 a trend towards greater canopy-linked soil CO<sub>2</sub> efflux was greater in the birch plots.  
508 However, the fact that this was not statistically significant may be related to the more rapid  
509 reduction in LAI within the willow plots.

510         The limited hyphal colonisation of the in-growth bags in both girdled and control  
511 willow plots suggests that willow shrubs do not rely significantly on ECM extramatrical  
512 mycelium for nutrient acquisition (although colonisation by smooth, contact type ECM fungi  
513 without extensive mycelial proliferation outside of the roots may take place (Agerer, 2001)).  
514 As outlined above, this may be due to a) greater soil moisture in the willow plots, and  
515 potential for anoxic conditions, having adverse effects on the fungi (Lodge, 1989;  
516 Wurzburger *et al.*, 2004; Barnes *et al.*, 2018), or b) drifting snow (Naito & Cairns, 2011)  
517 resulting in increased influx of dissolved and particulate compounds and/or increased  
518 mobilisation of nitrogen by the winter-active microbial community (Nadelhoffer *et al.*, 1991;  
519 Schimel *et al.*, 2004), and thus reducing investment in mycorrhizas by the shrubs. We  
520 propose that arctic willows, growing typically in moist topographies, may rely more on roots  
521 and direct uptake of nutrients, than on ECM fungi.

522 We have demonstrated that recent photosynthate regulates soil CO<sub>2</sub> efflux in  
523 subarctic forest communities beyond what is expected from the contribution of canopies to  
524 community LAI. Trees and shrubs are potential future land cover types on what is presently  
525 tundra heath (Pearson *et al.*, 2013) and some of the extra C that will be fixed as a result of  
526 increasing photosynthesis in these more productive ecosystems will be rapidly returned to  
527 the atmosphere through the rhizosphere. Unexpectedly, we found that birch and willow  
528 canopies contributed similarly large proportions to soil CO<sub>2</sub> efflux, but much more canopy-  
529 fixed C was allocated to mycorrhizal mycelium by birch. At present, our understanding of  
530 rhizosphere processes and subsequent C losses lags behind research on above-ground  
531 processes. Evidence from previous research suggests that rhizosphere priming of soil  
532 organic matter occurs in subarctic treeline forests and that forest expansion could even lead  
533 to a net loss of C from the ecosystem (Hartley *et al.*, 2012). The majority of tundra soils have  
534 scarce mineral nutrient availability (Shaver *et al.*, 1992), therefore greater investment  
535 below-ground by plants may be required to mobilise nutrients for further growth. If soil CO<sub>2</sub>  
536 efflux increases in tundra soils in response to increased plant growth, a critical research  
537 priority will be to understand what proportion of the increased efflux is short-term root  
538 respiration, and how much is the decomposition of soil organic matter in response to  
539 rhizosphere inputs.

540

#### 541 Acknowledgements

542 This work was funded by the Natural Environment Research Council (NERC) grant numbers  
543 NE/P002722/1 and NE/P002722/2 to PAW, DJ, JA-S and IPH. DJ received partial support  
544 from the N8 AgriFood programme. We warmly thank Ilona Kater, Gwen Lancashire, Ian  
545 Washbourne, Lea-Carlotta Kremp and Alyssa Parker for assistance in collecting field data.  
546 We thank staff of the Abisko Naturvetenskapliga Station for their assistance and logistical  
547 support.

548 **References**

549 **Agerer R. 2001.** Exploration types of ectomycorrhizae - A proposal to classify  
550 ectomycorrhizal mycelial systems according to their patterns of differentiation and putative  
551 ecological importance. *Mycorrhiza* **11**: 107–114.

552 **Barnes CJ, van der Gast CJ, McNamara NP, Rowe R, Bending GD. 2018.** Extreme rainfall  
553 affects assembly of the root-associated fungal community. *New Phytologist* **220**: 1172–  
554 1184.

555 **Bjerke JW, Karlsen SR, Hogda KA, Malnes E, Jepsen JU, Lovibond S, Vikhamar-Schuler D,**  
556 **Tommervik H. 2014.** Record-low primary productivity and high plant damage in the Nordic  
557 Arctic Region in 2012 caused by multiple weather events and pest outbreaks. *Environmental*  
558 *Research Letters* **9**.

559 **Bjorkman AD, Myers-Smith IH, Elmendorf SC, Normand S, R uger N, Beck PSA, Blach-**  
560 **Overgaard A, Blok D, Cornelissen JHC, Forbes BC, et al. 2018.** Plant functional trait change  
561 across a warming tundra biome. *Nature* **562**: 57–62.

562 **B odeker ITM, Clemmensen KE, de Boer W, Martin F, Olson  , Lindahl BD. 2014.**  
563 Ectomycorrhizal Cortinarius species participate in enzymatic oxidation of humus in northern  
564 forest ecosystems. *New Phytologist* **203**: 245–256.

565 **Bond-Lamberty B, Wang CK, Gower ST. 2004.** A global relationship between the  
566 heterotrophic and autotrophic components of soil respiration? *Global Change Biology* **10**:  
567 1756–1766.

568 **Clemmensen KE, Finlay RD, Dahlberg A, Stenlid J, Wardle DA, Lindahl BD. 2015.** Carbon  
569 sequestration is related to mycorrhizal fungal community shifts during long-term succession  
570 in boreal forests. *New Phytologist* **205**: 1525–1526.

571 **Demarco J, Mack MC, Bret-Harte MS. 2014.** Effects of arctic shrub expansion on biophysical  
572 vs. biogeochemical drivers of litter decomposition. *Ecology* **95**: 1861–1875.

573 **Drigo B, Anderson IC, Kannangara GSK, Cairney JWG, Johnson D. 2012.** Rapid incorporation  
574 of carbon from ectomycorrhizal mycelial necromass into soil fungal communities. *Soil*  
575 *Biology and Biochemistry* **49**: 4–10.

576 **Elmendorf SC, Henry GHR, Hollister RD, Bjork RG, Bjorkman AD, Callaghan T V, Collier LS,**  
577 **Cooper EJ, Cornelissen JHC, Day TA, et al. 2012a.** Global assessment of experimental  
578 climate warming on tundra vegetation: heterogeneity over space and time. *Ecology Letters*  
579 **15:** 164–175.

580 **Elmendorf SC, Henry GHR, Hollister RD, Bjork RG, Boulanger-Lapointe N, Cooper EJ,**  
581 **Cornelissen JHC, Day TA, Dorrepaal E, Elumeeva TG, et al. 2012b.** Plot-scale evidence of  
582 tundra vegetation change and links to recent summer warming. *Nature Climate Change* **2:**  
583 453–457.

584 **Epstein HE, Raynolds MK, Walker DA, Bhatt US, Tucker CJ, Pinzon JE. 2012.** Dynamics of  
585 aboveground phytomass of the circumpolar Arctic tundra during the past three decades.  
586 *Environmental Research Letters* **7:** 015506.

587 **Fernandez CW, Heckman K, Kolka R, Kennedy PG. 2019.** Melanin mitigates the accelerated  
588 decay of mycorrhizal necromass with peatland warming. *Ecology Letters* **22:** 498–505.

589 **Forbes BC, Macias Fauria M, Zetterberg P. 2010.** Russian Arctic warming and ‘greening’ are  
590 closely tracked by tundra shrub willows. *Global Change Biology* **16:** 1542–1554.

591 **Forrest AF. 2006.** Hybridization in sub-arctic willow scrub in Scotland.

592 **Hagedorn F, Shiyatov SG, Mazepa VS, Devi NM, Grigor’ev AA, Bartysh AA, Fomin V V,**  
593 **Kapralov DS, Terent’ev M, Bugman H, et al. 2014.** Treeline advances along the Urals  
594 mountain range – driven by improved winter conditions? *Global Change Biology* **20:** 3530–  
595 3543.

596 **Hagenbo A, Hadden D, Clemmensen KE, Grelle A, Manzoni S, Mölder M, Ekblad A,**  
597 **Fransson P. 2019.** Carbon use efficiency of mycorrhizal fungal mycelium increases during the  
598 growing season but decreases with forest age across a *Pinus sylvestris* chronosequence.  
599 *Journal of Ecology* **0.**

600 **Hagenbo A, Kyaschenko J, Clemmensen KE, Lindahl BD, Fransson P, Wurzbürger N. 2018.**  
601 Fungal community shifts underpin declining mycelial production and turnover across a *Pinus*  
602 *sylvestris* chronosequence. *Journal of Ecology* **106:** 490–501.

603 **Harsch MA, Hulme PE, McGlone MS, Duncan RP. 2009.** Are treelines advancing? A global

604 meta-analysis of treeline response to climate warming. *Ecology Letters* **12**: 1040–1049.

605 **Hartley IP, Garnett MH, Sommerkorn M, Hopkins DW, Fletcher BJ, Sloan VL, Phoenix GK,**  
606 **Wookey PA. 2012.** A potential loss of carbon associated with greater plant growth in the  
607 European Arctic. *Nature Climate Change* **2**: 875–879.

608 **Hasselquist NJ, Metcalfe DB, Högberg P. 2012.** Contrasting effects of low and high nitrogen  
609 additions on soil CO<sub>2</sub> flux components and ectomycorrhizal fungal sporocarp production in  
610 a boreal forest. *Global Change Biology* **18**: 3596–3605.

611 **Heinemeyer A, Hartley IP, Evans SP, De la Fuente JAC, Ineson P. 2007.** Forest soil CO<sub>2</sub> flux:  
612 uncovering the contribution and environmental responses of ectomycorrhizas. *Global*  
613 *Change Biology* **13**: 1786–1797.

614 **Heliasz M, Johansson T, Lindroth A, Molder M, Mastepanov M, Friborg T, Callaghan T V,**  
615 **Christensen TR. 2011.** Quantification of C uptake in subarctic birch forest after setback by an  
616 extreme insect outbreak. *Geophysical Research Letters* **38**.

617 **Hicks Pries CE, van Logtestijn RSP, Schuur EAG, Natali SM, Cornelissen JHC, Aerts R,**  
618 **Dorrepaal E. 2015.** Decadal warming causes a consistent and persistent shift from  
619 heterotrophic to autotrophic respiration in contrasting permafrost ecosystems. *Global*  
620 *change biology* **21**: 4508–4519.

621 **Hofgaard A, Tommervik H, Rees G, Hanssen F. 2013.** Latitudinal forest advance in  
622 northernmost Norway since the early 20th century. *Journal of Biogeography* **40**: 938–949.

623 **Högberg P, Nordgren A, Buchmann N, Taylor AFS, Ekblad A, Högberg MN, Nyberg G,**  
624 **Ottosson-Lofvenius M, Read DJ. 2001.** Large-scale forest girdling shows that current  
625 photosynthesis drives soil respiration. *Nature* **411**: 789–792.

626 **Iversen CM, Sloan VL, Sullivan PF, Euskirchen ES, McGuire AD, Norby RJ, Walker AP,**  
627 **Warren JM, Wullschleger SD. 2015.** Tansley review The unseen iceberg : plant roots in arctic  
628 tundra. *New Phytologist* **205**: 34–58.

629 **Jackson RB, Canadell J, Ehleringer JR, Mooney HA, Sala OE, Schulze ED. 1996.** A global  
630 analysis of root distributions for terrestrial biomes. *Oecologia* **108**: 389–411.

631 **Kritzler UH, Artz RRE, Johnson D. 2016.** Soil CO<sub>2</sub> efflux in a degraded raised bog is regulated

632 by water table depth rather than recent plant assimilate. *Mires and Peat* **17**: 1–14.

633 **Kuhry P, Grosse G, Harden JW, Hugelius G, Koven CD, Ping CL, Schirrmeister L, Tarnocai C.**  
634 **2013.** Characterisation of the permafrost carbon pool. *Permafrost and Periglacial Processes*  
635 **24**: 146–155.

636 **Kulmala L, Pumpanen J, Kolari P, Dengel S, Berninger F, Köster K, Matkala L, Vanhatalo A,**  
637 **Vesala T, Bäck J. 2019.** Inter- and intra-annual dynamics of photosynthesis differ between  
638 forest floor vegetation and tree canopy in a subarctic Scots pine stand. *Agricultural and*  
639 *Forest Meteorology* **271**: 1–11.

640 **Kuzyakov Y. 2002.** Review: Factors affecting rhizosphere priming effects. *Journal of Plant*  
641 *Nutrition and Soil Science-Zeitschrift Fur Pflanzenernahrung Und Bodenkunde* **165**: 382–396.

642 **Lindahl BD, Tunlid A. 2015.** Ectomycorrhizal fungi – potential organic matter decomposers,  
643 yet not saprotrophs. *New Phytologist* **205**: 1443–1447.

644 **Lodge DJ. 1989.** The influence of soil moisture and flooding on formation of VA-endo- and  
645 ectomycorrhizae in *Populus* and *Salix*. *Plant and Soil* **117**: 243–253.

646 **Myers-Smith IH, Forbes BC, Wilmking M, Hallinger M, Lantz T, Blok D, Tape KD, Macias-**  
647 **Fauria M, Sass-Klaassen U, Levesque E, et al. 2011.** Shrub expansion in tundra ecosystems:  
648 dynamics, impacts and research priorities. *Environmental Research Letters* **6**: 045509.

649 **Myers-Smith IH, Grabowski MM, Thomas HJD, Angers-Blondin S, Daskalova GN, Bjorkman**  
650 **AD, Cunliffe AM, Assmann JJ, Boyle JS, McLeod E, et al. 2019a.** Eighteen years of ecological  
651 monitoring reveals multiple lines of evidence for tundra vegetation change. *Ecological*  
652 *Monographs* **89**: e01351.

653 **Myers-Smith IH, Kerby JT, Phoenix GK, Bjerke JW, Epstein HE, Assmann JJ, John C, Andreu-**  
654 **Hayles L, Angers-Blondin S, Beck PSA, et al. 2020.** Complexity revealed in the greening of  
655 the Arctic. *Nature Climate Change* **10**: 106–117.

656 **Myers-Smith IH, Thomas HJD, Bjorkman AD. 2019b.** Plant traits inform predictions of  
657 tundra responses to global change. *New Phytologist* **221**: 1742–1748.

658 **Nadelhoffer KJ, Giblin AE, Shaver GR, Laundre JA. 1991.** Effects of temperature and  
659 substrate quality on element mineralization in 6 arctic soils. *Ecology* **72**: 242–253.



660 **Naito AT, Cairns DM. 2011.** Relationships between Arctic shrub dynamics and  
661 topographically derived hydrologic characteristics. *Environmental Research Letters* **6**:  
662 045506.

663 **Palacio S, Hester AJ, Maestro M, Millard P. 2008.** Browsed *Betula pubescens* trees are not  
664 carbon-limited. *Functional Ecology* **22**: 808–815.

665 **Parker TC, Sadowsky J, Dunleavy H, Subke J-A, Frey SD, Wookey PA. 2017.** Slowed  
666 Biogeochemical Cycling in Sub-arctic Birch Forest Linked to Reduced Mycorrhizal Growth  
667 and Community Change after a Defoliation Event. *Ecosystems* **20**: 316–330.

668 **Parker TC, Sanderman J, Holden RD, Blume-Werry G, Sjögersten S, Large D, Castro-Díaz M,  
669 Street LE, Subke J-A, Wookey PA. 2018.** Exploring drivers of litter decomposition in a  
670 greening Arctic: results from a transplant experiment across a treeline. *Ecology* **99**: 2284–  
671 2294.

672 **Parker TC, Subke J-A, Wookey PA. 2015.** Rapid carbon turnover beneath shrub and tree  
673 vegetation is associated with low soil carbon stocks at a subarctic treeline. *Global Change  
674 Biology* **21**: 2070–81.

675 **Pearson RG, Phillips SJ, Lorant MM, Beck PSA, Damoulas T, Knight SJ, Goetz SJ. 2013.**  
676 Shifts in Arctic vegetation and associated feedbacks under climate change. *Nature Climate  
677 Change* **3**: 673–677.

678 **Pérez-Izquierdo L, Clemmensen KE, Strengbom J, Nilsson M-C, Lindahl BD. 2019.**  
679 Quantification of tree fine roots by real-time PCR. *Plant and Soil* **440**: 440–593.

680 **Pinheiro J, Bates D, DebRoy S, Sarkar D, R Core Team. 2016.** {nlme}: Linear and Nonlinear  
681 Mixed Effects Models.

682 **Qian H, Joseph R, Zeng N. 2010.** Enhanced terrestrial carbon uptake in the Northern High  
683 Latitudes in the 21st century from the Coupled Carbon Cycle Climate Model  
684 Intercomparison Project model projections. *Global Change Biology* **16**: 641–656.

685 **R Development Core Team. 2016.** R: A Language and Environment for Statistical Computing.

686 **Reichle LM, Epstein HE, Bhatt US, Reynolds MK, Walker DA. 2018.** Spatial Heterogeneity of  
687 the Temporal Dynamics of Arctic Tundra Vegetation. *Geophysical Research Letters* **45**: 9206–

688 9215.

689 **Richardson AD, Friedland AJ. 2009.** A Review of the Theories to Explain Arctic and Alpine  
690 Treelines Around the World. *Journal of Sustainable Forestry* **28**: 218–242.

691 **Rouse J, Haas R, Schell J, Deering D. 1974.** *Monitoring vegetation systems in the Great*  
692 *Plains with ERTS*. Washington, DC.

693 **Schimel JP, Bilbrough C, Welker JA. 2004.** Increased snow depth affects microbial activity  
694 and nitrogen mineralization in two Arctic tundra communities. *Soil Biology & Biochemistry*  
695 **36**: 217–227.

696 **Shaver GR, Billings WD, Chapin FS, Giblin AE, Nadelhoffer KJ, Oechel WC, Rastetter EB.**  
697 **1992.** Global Change and the Carbon Balance of Arctic Ecosystems. *BioScience* **42**: 433–441.

698 **Shaver GR, Street LE, Rastetter EB, Van Wijk MT, Williams M. 2007.** Functional  
699 convergence in regulation of net CO<sub>2</sub> flux in heterogeneous tundra landscapes in Alaska  
700 and Sweden. *Journal of Ecology* **95**: 802–817.

701 **Siewert MB. 2018.** High-resolution digital mapping of soil organic carbon in permafrost  
702 terrain using machine learning: a case study in a sub-Arctic peatland environment.  
703 *Biogeosciences* **15**: 1663–1682.

704 **Siewert MB, Hanisch J, Weiss N, Kuhry P, Maximov TC, Hugelius G. 2015.** Comparing  
705 carbon storage of Siberian tundra and taiga permafrost ecosystems at very high spatial  
706 resolution. *Journal of Geophysical Research: Biogeosciences* **120**: 1973–1994.

707 **Sjögersten S, Wookey P a. 2002.** Climatic and resource quality controls on soil respiration  
708 across a forest-tundra ecotone in Swedish Lapland. *Soil Biology and Biochemistry* **34**: 1633–  
709 1646.

710 **Söderström B, Read DJ. 1987.** Respiratory activity of intact and excised ectomycorrhizal  
711 mycelial systems growing in unsterilized soil. *Soil Biology and Biochemistry* **19**: 231–236.

712 **Sørensen MV, Strimbeck R, Nystuen KO, Kapas RE, Enquist BJ, Graae BJ. 2018.** Draining the  
713 Pool? Carbon Storage and Fluxes in Three Alpine Plant Communities. *Ecosystems* **21**: 316–  
714 330.

715 **Sterkenburg E, Clemmensen KE, Ekblad A, Finlay RD, Lindahl BD. 2018.** Contrasting effects

716 of ectomycorrhizal fungi on early and late stage decomposition in a boreal forest. *The ISME*  
717 *Journal* **12**: 2187–2197.

718 **Street LE, Shaver GR, Williams M, Van Wijk MT. 2007.** What is the relationship between  
719 changes in canopy leaf area and changes in photosynthetic CO<sub>2</sub> flux in arctic ecosystems?  
720 *Journal of Ecology* **95**: 139–150.

721 **Street LE, Subke J-A, Baxter R, Dinsmore KJ, Knoblauch C, Wookey PA. 2018.** Ecosystem  
722 carbon dynamics differ between tundra shrub types in the western Canadian Arctic.  
723 *Environmental Research Letters* **13**: 84014.

724 **Sturm M, Schimel J, Michaelson G, Welker JM, Oberbauer SF, Liston GE, Fahnestock J,**  
725 **Romanovsky VE. 2005.** Winter biological processes could help convert arctic tundra to  
726 shrubland. *BioScience* **55**: 17–26.

727 **Subke J-A, Inglima I, Cotrufo MF. 2006.** Trends and methodological impacts in soil CO<sub>2</sub>  
728 efflux partitioning: A metaanalytical review. *Global Change Biology* **12**: 921–943.

729 **Sullivan P, Sommerkorn M, Rueth H. 2007.** Climate and species affect fine root production  
730 with long-term fertilization in acidic tussock tundra near Toolik Lake, Alaska. *Oecologia* **153**:  
731 643–652.

732 **Tape K, Sturm M, Racine C. 2006.** The evidence for shrub expansion in Northern Alaska and  
733 the Pan-Arctic. *Global Change Biology* **12**: 686–702.

734 **Treseder KK. 2004.** A meta-analysis of mycorrhizal responses to nitrogen, phosphorus, and  
735 atmospheric CO<sub>2</sub> in field studies. *New Phytologist* **164**: 347–355.

736 **Walker DA, Reynolds MK, Daniëls FJA, Einarsson E, Elvebakk A, Gould WA, Katenin AE,**  
737 **Kholod SS, Markon CJ, Melnikov ES, et al. 2005.** The Circumpolar Arctic vegetation map.  
738 *Journal of Vegetation Science* **16**: 267–282.

739 **Wallander H, Ekblad A, Godbold DL, Johnson D, Bahr A, Baldrian P, Bjork RG, Kieliszewska-**  
740 **Rokicka B, Kjoller R, Kraigher H, et al. 2013.** Evaluation of methods to estimate production,  
741 biomass and turnover of ectomycorrhizal mycelium in forests soils - A review. *Soil Biology &*  
742 *Biochemistry* **57**: 1034–1047.

743 **Wardle DA, Jonsson M, Bansal S, Bardgett RD, Gundale MJ, Metcalfe DB. 2012.** Linking

744 vegetation change, carbon sequestration and biodiversity: insights from island ecosystems  
745 in a long-term natural experiment. *Journal of Ecology* **100**: 16–30.

746 **Wilkinson A, Alexander IJ, Johnson D. 2011.** Species richness of ectomycorrhizal hyphal  
747 necromass increases soil CO<sub>2</sub> efflux under laboratory conditions. *Soil Biology and*  
748 *Biochemistry* **43**: 1350–1355.

749 **Williams M, Bell R, Spadavecchia L, Street LE, Van Wijk MT. 2008.** Upscaling leaf area index  
750 in an Arctic landscape through multiscale observations. *Global Change Biology* **14**: 1517–  
751 1530.

752 **Wilmking M, Harden J, Tape K. 2006.** Effect of tree line advance on carbon storage in NW  
753 Alaska. *Journal of Geophysical Research-Biogeosciences* **111**: G02023.

754 **Wurzburger N, Hartshorn AS, Hendrick RL. 2004.** Ectomycorrhizal fungal community  
755 structure across a bog-forest ecotone in southeastern Alaska. *Mycorrhiza* **14**: 383–389.

756 **Yu Q, Epstein H, Engstrom R, Walker D. 2017.** Circumpolar arctic tundra biomass and  
757 productivity dynamics in response to projected climate change and herbivory. *Global*  
758 *Change Biology* **23**: 3895–3907.

759 **Zak DR, Pellitier PT, Argiroff WA, Castillo B, James TY, Nave LE, Averill C, Beidler K,**  
760 **Bhatnagar J, Blesh J, et al. 2019.** Exploring the role of ectomycorrhizal fungi in soil carbon  
761 dynamics. *New Phytologist* **223**: 33–39.

762

763

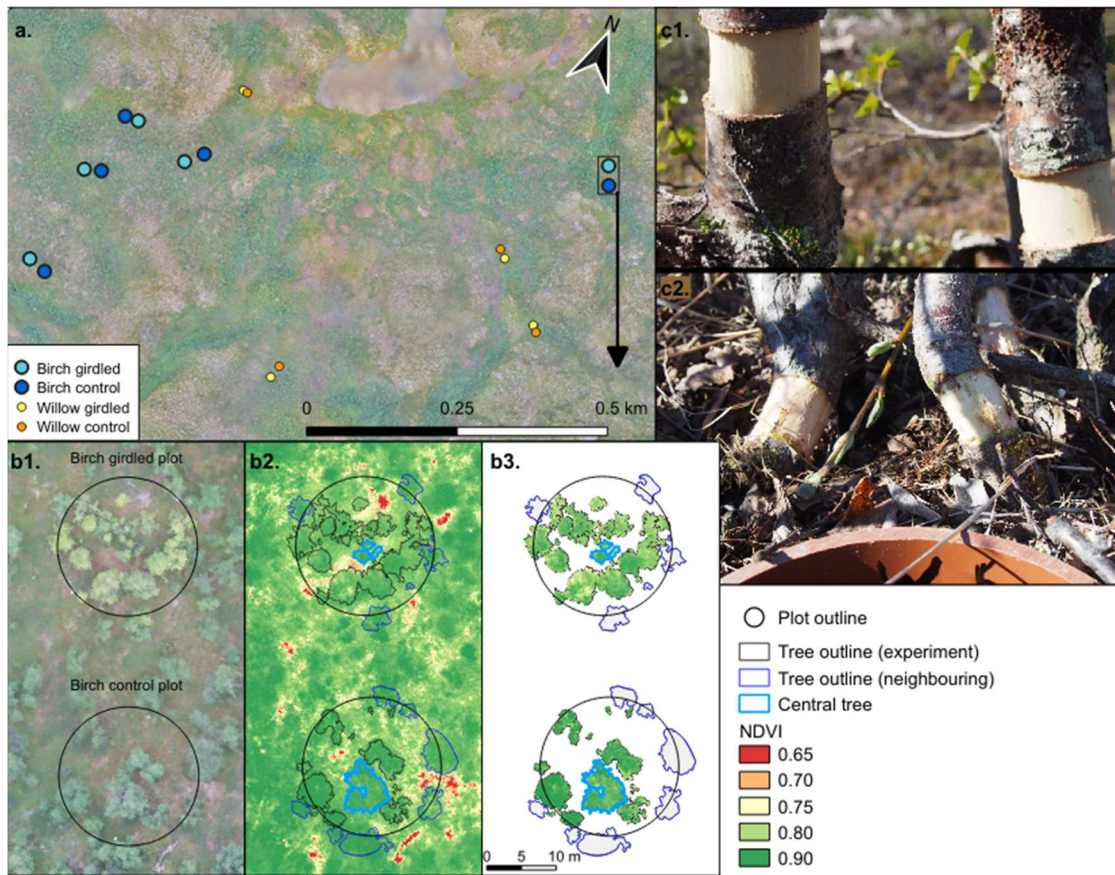
764 Table 1: Average ( $\pm 1$  standard error) vegetation and soil characteristics in control and  
 765 girdled plots of birch (n = 6 pairs) and willow (n = 5 pairs). Soil respiration values are for  
 766 measurement days prior to implementation of the girdling treatment.

	Birch		Willow	
	Control	Girdled	Control	Girdled
Trees (Trees ha <sup>-1</sup> )	573 $\pm$ 72.1	600 $\pm$ 83.6		
Stems (Stems m <sup>-2</sup> )	0.27 $\pm$ 0.03	0.20 $\pm$ 0.01	5.98 $\pm$ 0.45	5.52 $\pm$ 0.43
Canopy height (cm)			82.7 $\pm$ 9.26	76.7 $\pm$ 8.57
Organic horizon SOC (kg m <sup>-2</sup> )	2.80 $\pm$ 0.17	2.57 $\pm$ 0.20	3.07 $\pm$ 0.46	2.50 $\pm$ 0.35
Soil C:N ratio	29.6 $\pm$ 1.02	28.7 $\pm$ 1.33	25.0 $\pm$ 0.38	25.6 $\pm$ 1.09
Soil CO <sub>2</sub> efflux ( $\mu\text{mol m}^{-2} \text{s}^{-1}$ )	2.80 $\pm$ 0.15	2.59 $\pm$ 0.18	2.48 $\pm$ 0.34	2.37 $\pm$ 0.10

767

768 Table 2: Mean ( $\pm 1$  SE) root and hyphae production over full growing seasons, canopy LAI, and understorey Normalised Difference Vegetation  
 769 Index (NDVI) in late July in birch and willow, girdled and control plots (Birch = 6 paired plots, Willow = 5 paired plots) in 2017 and 2018. Root  
 770 production values are from the top 6 cm of soil, hyphae production from the top 3.5 cm of soil. Test statistics from linear mixed effects models  
 771 for fixed effects (species, treatment, and the interaction, if present) for each response variable in each year are provided in line.

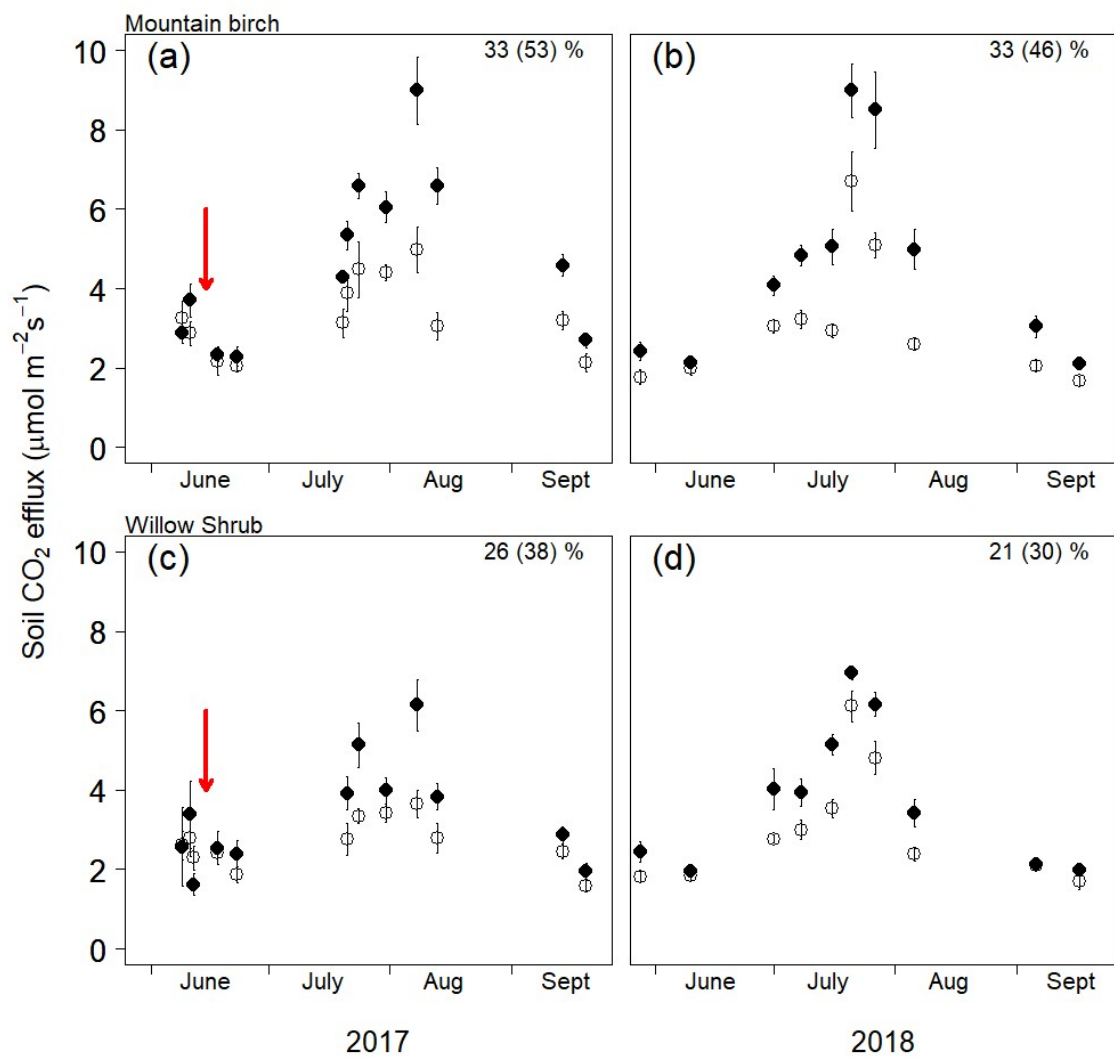
	Birch Forest				Willow Shrub				Species			Treatment			Species x Treatment		
	Control		Girdled		Control		Girdled		d.f.	F	P	d.f.	F	P	d.f.	F	P
<b>2017</b>																	
Roots (mg C bag <sup>-1</sup> )	11.5	$\pm$ 3.79	2.75	$\pm$ 0.83	6.30	$\pm$ 1.15	4.37	$\pm$ 1.27	1,9	0.05	0.829	1,9	11.1	0.009	1,9	2.50	0.148
Birch ITS copies (bag <sup>-1</sup> )	6032	$\pm$ 3678	180	$\pm$ 116								1,3	6.87	0.079			
Hyphae (mg C bag <sup>-1</sup> )	1.07	$\pm$ 0.39	0.19	$\pm$ 0.07	0.11	$\pm$ 0.03	0.24	$\pm$ 0.13	1,9	4.64	0.060	1,9	1.35	0.275	1,9	0.95	0.356
Canopy LAI (m <sup>2</sup> m <sup>-2</sup> )	0.50	$\pm$ 0.21	0.58	$\pm$ 0.23	1.51	$\pm$ 0.50	0.56	$\pm$ 0.15	1,9	0.41	0.537	1,9	3.87	0.081	1,9	3.93	0.079
Canopy NDVI	0.87	$\pm$ 0.01	0.85	$\pm$ 0.01	0.83	$\pm$ 0.01	0.77	$\pm$ 0.01	1,9	47.41	< 0.001	1,9	122	< 0.001	1,9	32.94	< 0.001
Understorey NDVI	0.81	$\pm$ 0.02	0.81	$\pm$ 0.01								1,5	0.14	0.724			
<b>2018</b>																	
Roots (mg C bag <sup>-1</sup> )	8.84	$\pm$ 2.19	7.15	$\pm$ 1.55	17.41	$\pm$ 5.79	7.68	$\pm$ 2.48	1,9	1.48	0.255	1,9	2.90	0.123	1,9	0.84	0.383
Birch ITS copies (bag <sup>-1</sup> )	30000	$\pm$ 25317	18	$\pm$ 17								1,5	24.72	0.004			
Hyphae (mg C bag <sup>-1</sup> )	2.43	$\pm$ 0.87	0.02	$\pm$ 0.01	0.32	$\pm$ 0.18	0.18	$\pm$ 0.06	1,9	1.30	0.284	1,9	28.86	< 0.001	1,9	21.58	0.001
LAI (m <sup>2</sup> m <sup>-2</sup> )	0.92	$\pm$ 0.10	0.65	$\pm$ 0.07								1,5	10.33	0.024			
Canopy NDVI	0.81	$\pm$ 0.01	0.74	$\pm$ 0.01	0.72	$\pm$ 0.01	0.65	$\pm$ 0.02	1,9	39.92	< 0.001	1,9	68.33	< 0.001	1,9	0.29	0.606
Understorey NDVI	0.74	$\pm$ 0.02	0.74	$\pm$ 0.02								1,5	0.00	0.964			



773

774 Figure 1: (a) Location of paired girdled and control plots of birch (blue circles) and willow  
 775 (orange circles) at field sites south of Abisko (note that 1 birch pair and 1 willow pair are 200  
 776 m south, out-with the image). (b) Birch pair 6 with plot perimeters superimposed (b1), false  
 777 colour imagery of NDVI values and trees within the experiment marked (b2) and  
 778 experimental and central study tree only marked (b3). (c) Examples of stem girdling in birch  
 779 plots (c1) and willow plots (c2).

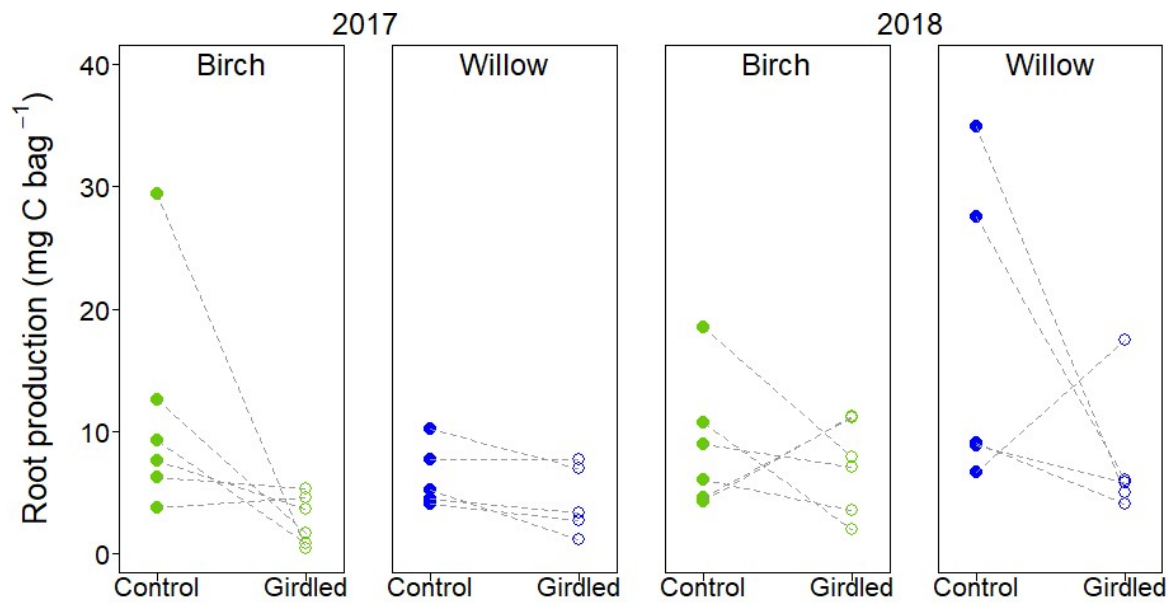
780



781

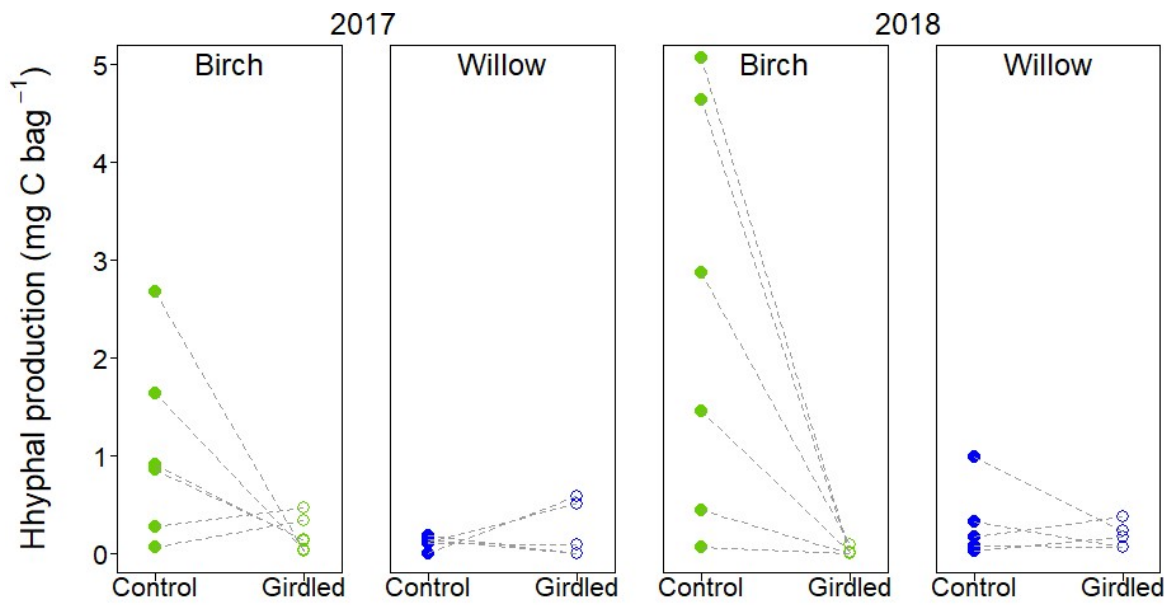
782 Figure 2: Soil CO<sub>2</sub> efflux from Mountain birch in 2017 (a) and 2018 (b), and Willow shrub in  
 783 2017 (c) and 2018 (d) in control (filled circles) and girdled plots (open circles). Points  
 784 represent mean values at each sampling date ( $\pm 1$  standard error). Arrows (red) indicate the  
 785 date of girdling in the respective communities. In 2017 there were significant effects of  
 786 species ( $F_{(1,9)} = 14.0$ ,  $P = 0.005$ ), girdling treatment ( $F_{(1,10)} = 24.3$ ,  $P < 0.001$ ) and season  
 787 ( $F_{(1,186)} = 130$ ,  $P < 0.001$ ) and no interactions between species and treatment ( $F_{(1,9)} = 0.59$ ,  $P =$   
 788  $0.46$ ). In 2018 there was no significant effect of species ( $F_{(1,9)} = 3.24$ ,  $P = 0.11$ ) but effects of  
 789 girdling treatment ( $F_{(1,10)} = 36.7$ ,  $P < 0.001$ ) and season ( $F_{(2,196)} = 168$ ,  $P < 0.001$ ); there was no  
 790 interaction between species and treatment ( $F_{(1,9)} = 2.00$ ,  $P = 0.19$ ). The percentage  
 791 contributions of the canopy to soil CO<sub>2</sub> efflux over the over the whole growing season and at  
 792 its seasonal maximum (in brackets) are reported in the top right of each panel.





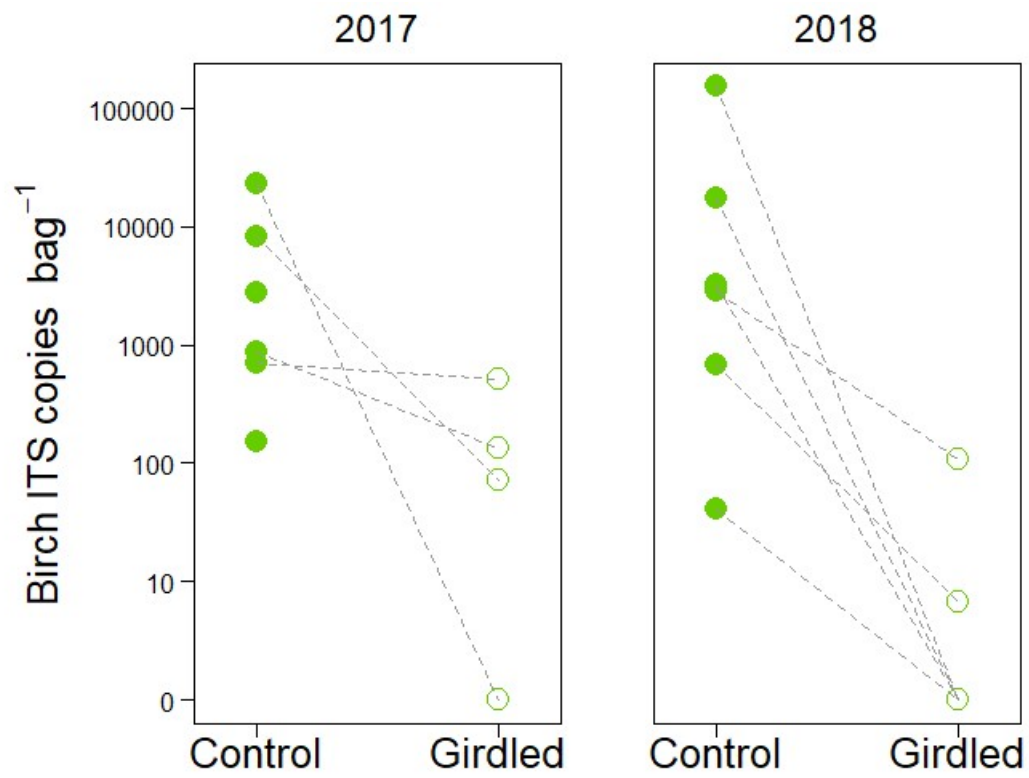
794

795 Figure 3: Root production (mass of C into ingrowth bag) in paired (denoted by dashed  
 796 connecting lines) control and girdled plots in 2017 and 2018 in birch (green) and willow  
 797 (blue) plots. The results of statistical analyses are shown in Table 2.



799

800 Figure 4: Hyphal production (mass of C into ingrowth bag) in paired (denoted by dashed  
 801 connecting lines) control and girdled plots in 2017 and 2018 in birch (green) and willow  
 802 (blue) plots. The results of statistical analyses are shown in Table 2.



803

804 Figure 5: Birch ITS copy numbers in ingrowth bags in paired (denoted by dashed connecting  
 805 lines) birch girdled and control plots in 2017 and 2018. The results of statistical analyses are  
 806 shown in Table 2.

807

808